Cancer Chemother Pharmacol (1996) 39: 51–60

ORIGINAL ARTICLE

Merrill J. Egorin · Dorothy L. Sentz · D. Marc Rosen
Michael F. Ballesteros · Christine M. Kearns
Patrick S. Callery · Julie L. Eiseman

Plasma pharmacokinetics, bioavailability, and tissue distribution in CD_2F_1 mice of halomon, an antitumor halogenated monoterpene isolated from the red algae *Portieria hornemannii*

Received: 18 February 1996/Accepted: 13 June 1996

Abstract The purpose of the present study was to define the plasma pharmacokinetics, bioavailability, and tissue distribution in mice of halomon, a halogenated monoterpene from *Portieria hornemanii* that is active in vitro against brain-, renal-, and colon-cancer cell lines. Halomon formulated in cremophor : ethanol : 0.154 *M* NaCl (1 : 1 : 6, by vol.) was injected i.v. at 20, 60, 90, or 135 mg/kg into female CD_2F_1 mice. Doses of 135 mg/kg were also given i.p., s.c., and by enteral gavage to female CD_2F_1 mice and i.v. to male CD_2F_1 mice. Plasma halomon concentrations were measured with a gas-chromatography system using electron-capture detection. Halomon concentrations were also determined in the brains, hearts, lungs, livers, kidneys, spleens, skeletal muscles, fat, red blood cells, and, if present, testes of mice given 135 mg/kg i.v. Halomon plasma pharmacokinetics were well fit by a two-compartment, open linear model and were linear between 20 and 135 mg/kg. Population estimates of parameters describing halomon plasma pharmacokinetics in female CD_2F_1 mice were developed with a standard two-stage technique and also by simultaneous modeling of data from 20-, 60-, 90-, and 135-mg/kg i.v. studies in female mice. Halomon bioavailability was 45%, 47%, and 4% after i.p., s.c., and enteral dosing, respectively. Urinary excretion of the parent compound was minimal. Halomon was distributed widely to all tissues studied but was concentrated and persisted in fat. Halomon concentrations measured in the brain were comparable with concomitant concentrations detected in plasma and most other tissues. These data and models are helpful in the simulation and evaluation of conditions produced by preclinical screening and toxicology studies.

Key words Halomon · Natural products · Halogenated monoterpenes · Pharmacokinetics

This work was supported by contracts N01-CM27711 and N01-CM27199, awarded by the National Cancer Institute

M.J. Egorin (✉) · D.L. Sentz · D.M. Rosen · M.F. Ballesteros
C.M. Kearns · P.S. Callery · J.L. Eiseman
Division of Developmental Therapeutics, University of Maryland Cancer Center, Bressler 9-024, 655 West Baltimore Street, Baltimore, MD 21201, USA

M.J. Egorin · C.M. Kearns
Division of Hematology/Oncology, Department of Medicine, University of Maryland School of Medicine, Baltimore, MD 21201, USA

C.M. Kearns
Department of Pharmacy Practice and Science, University of Maryland School of Pharmacy, Baltimore, MD 21201, USA

P.S. Callery
Department of Pharmaceutical Sciences, University of Maryland School of Pharmacy, Baltimore, MD 21201, USA

J.L. Eiseman
Department of Pathology, University of Maryland School of Medicine, Baltimore, MD 21201 USA

Introduction

Rhodophyta (red algae) are known to produce halogenated monoterpenes [24]. One of these, 6(R)-bromo-3(S)-(bromomethyl)-7-methyl-2,3,7-trichloro-1-octene [halomon (NSC 650893); Fig. 1], has been isolated from the red algae *Portieria hornemannii* [12] and has demonstrated interesting activity when tested in the National Cancer Institute's (NCI's) human tumor, disease-oriented in vitro screen [11]. When analyzed by computerized pattern recognition using the COMPARE algorithm [4, 21], these in vitro studies indicated that the mechanism of action of halomon was different from that of a typical electrophilic alkylating agent. In addition, the screening profile of halomon bore no substantial resemblance to that of any known mechanistic or structural class of cytotoxic agent in the NCI data base. Moreover, the observation that cell

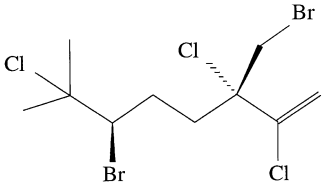

6(R)-Bromo-3(S)-bromomethyl-7-methyl-2,3,7-trichloro-1-octene

Halomon

Fig. 1 Chemical structure of halomon

lines that were relatively more sensitive to halomon clustered among renal, brain, colon, and non-small-cell lung cancer panels and those cell lines that were relatively less sensitive clustered among leukemia and melanoma panels was highly unusual.

The combination of a potentially unique mechanism of action and preferential cytotoxicity to cell lines derived from highly chemoresistant human tumors led to in vivo evaluation of the antitumor activity of halomon. As part of the continued development of this interesting natural product, studies were undertaken (1) to develop an analytical methodology for the measurement of halomon in biological matrices, (2) to perform pharmacokinetic studies in mice that had received halomon at a variety of doses and by several routes of administration, and (3) to develop pharmacokinetic models useful for the simulation and prediction of concentrations of halomon produced by dosing schedules and routes used in in vivo activity and toxicology studies. Those studies form the basis of this report.

Materials and methods

Reagents

Halomon and diluent 12, a 1 : 1 mixture of cremophor : ethanol, were obtained from the Developmental Therapeutics Program, NCI (Bethesda, Md.). Sesame oil and (+)-3,9-dibromocamphor (internal standard) were obtained from Sigma Chemical Co. (St. Louis, Mo.). Toluene, Baker analyzed grade, was obtained from J.T. Baker (Phillipsburg, N.J.). Halomon was initially dissolved to a concentration of 54 mg/ml in diluent 12 and then diluted further with sterile 0.154 *M* NaCl to a final concentration of 13.5 mg/ml. With this solution, halomon was delivered in a volume of 10 ml/kg body weight and at a dose of 135 mg/kg by the i.v., i.p. or s.c. route. For studies in which halomon was given i.v. at doses of 20, 60, or 90 mg/kg the drug was dissolved in diluent 12 : 0.154 *M* NaCl (1 : 3, v : v) such that the desired dose could be delivered in a volume of 10 ml/kg body weight. In the pharmacokinetics study using enteral administration of halomon, sterile, pyrogen-free, distilled water was substituted for NaCl as the diluent. In an additional study, halomon was mixed with sesame oil at a ratio of 13.5 mg/ml and was given i.p. such that the volume of sesame oil was 10 ml/kg body weight.

Mice

Specific-pathogen-free adult CD_2F_1 mice (5–6 weeks of age) were obtained from the Animal Program administered by the Animal Genetics and Production Branch of the NCI. Mice were allowed to acclimate to the University of Maryland Animal Facility for at least 1 week before studies were initiated. To minimize exogenous infection, mice were maintained in conventional cages in a separate room and were handled in accordance with the National Institutes of Heath (NIH) Guide for the Care and Use of Laboratory Animals (NIH number 85–23, 1985). Ventilation and air flow in the animal facility were set to 12 changes/h. Room temperatures were regulated at $72 \pm 2\,^{\circ}F$, and the rooms were on automatic 12-h light/dark cycles. Mice received Purina 5001 Chow and water ad libitum except on the evening prior to dosing, when all food was removed and withheld until 4 h after dosing. Sentinel mice (CD-1 mice housed in cages containing one-fifth bedding removed from the cages of study mice at cage change) were maintained in the animal room and were assayed at monthly intervals for specific murine pathogens by the murine antibody propile (MAP) test (Litton Bionetics, Charleston, S.C.). These mice remained free of specific pathogens throughout the study period, indicating that study mice were also free of specific pathogens. Both male and female mice were given i.v. doses of 135 mg/kg; however, in all other studies, only female mice were used. Three mice per dose group were studied at each time point.

Halomon administration

For i.v. administration, doses of halomon were given as boluses through a tail vein. Halomon was injected via other parenteral routes as a rapid bolus. The oral dose of halomon was delivered with a 22-gange gavage needle.

Sampling

In all studies, blood was sampled at 5, 10, 15, 30, 45, 60, 90, 120, 180, 240, 360, 480, 960, and 1,440 min after dosing. In studies in which halomon was injected i.v. at 135 mg/kg, brains, hearts, lungs, livers, kidneys, spleens, fat, skeletal muscles, and, in males, testicles were collected at the same times noted for blood samples. In addition, packed erythrocytes resulting from preparation of plasma were sampled in female mice at each time indicated. In each study, blood and tissues from mice killed 5 min after delivery of the diluent 12 and 0.154 *M* NaCl vehicle served as controls. Blood was collected by cardiac puncture into heparinized syringes, transferred to Eppendorf microcentrifuge tubes, and stored on ice until centrifuged at 13,000 *g* for 5 min to obtain plasma. Tissues were rapidly dissected, placed on ice until weighed, and then snap-frozen in liquid nitrogen. Sets of animals to be sampled at 960 or 1,440 min after dosing were gang-housed in metabolism cages, and urine was collected on ice until animals were killed for blood and, if necessary, tissue sampling. Plasma, tissues, urine, and dosing solutions were stored frozen at $-70\,^{\circ}C$ until analyzed.

Analysis of halomon

Plasma and tissue concentrations of halomon were determined by gas chromatography. Briefly, 100-µl samples of plasma were placed into Eppendorf microcentrifuge tubes, and 10 µl of internal standard was added to each tube. The internal standard consisted of a 4-µg/ml solution of (+)-3,9-dibromocamphor in 50% methanol. The tubes were vortexed, 100 µl of toluene was added to each tube, and the tubes were then shaken for 20 min on a Vortex Genie 2 (Model G-560, Scientific Industries, Inc., Bohemia, N.Y.) set at position 4. After being shaken, tubes were centrifuged at 13,000 *g* for 5 min and the resulting upper organic layer was transferred with a glass Pasteur pipet into glass microvial inserts. Then, 1 µl of the organic layer was injected by autosampler into the gas-chromatography system described below.

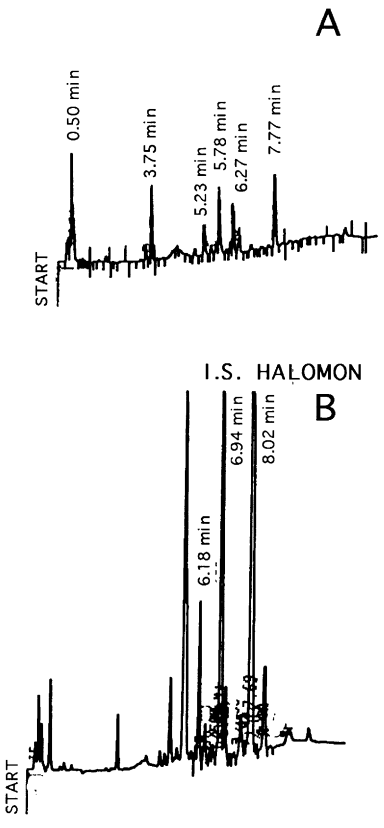

Fig. 2 A, B Gas chromatographic tracings of **A** control mouse plasma and **B** plasma obtained from a mouse 15 min after an i.v. bolus injection of halomon at a dose of 135 mg/kg

Tissue samples were thawed, immediately transferred to 17 × 100-mm polypropylene tubes that were held in an ice bath, and homogenized using a Polytron device (Brinkman Instruments, Westbury, N.Y.) in 3 parts (weight to volume) of phosphate-buffered saline (1.2 m*M* KH_2PO_4, 2.9 m*M* Na_2HPO_4, 154 m*M* NaCl, pH 7.4; Biofluids, Inc., Rockville, Md.). Next, 100 µl of each homogenate was placed into Eppendorf microcentrifuge tubes, mixed with 10 µl of internal standard, extracted with toluene, and prepared for injection into the gas chromatograph as described for plasma samples.

Toluene extracts were analyzed with a Hewlett-Packard 5890 gas chromatograph (Hewlett-Packard, Palo Alto, Calif.) fitted with a 10-m HP-5 (cross-linked 5% phenylmethylsilicone) column (0.53-mm inside diameter 2.65-µm film thickness) and equipped with a Hewlett-Packard 7673A autosampler. Injection was splitless with a purge time of 1 min, and the injector port was maintained at 250 °C. The oven temperature was maintained at 100 °C for 1 min and then increased at 20 °C/min to 250 °C, which was held for 3 min. The carrier gas was helium (at 3 psig) and the make-up gas was argon : methane (95 : 5). The column effluent was monitored with an electron-capture detector maintained at 300 °C, and the detector signal was processed with a Hewlett-Packard 3392A integrator so as to integrate the area under each peak. Under these conditions the retention times of the internal standard and halomon were approximately 6.94 and 8.02 min, respectively (Fig. 2). The halomon concentration in each sample was calculated by determining the ratio of the halomon peak area to that of the corresponding internal standard peak and comparing that ratio to a concomitantly performed standard curve prepared in the appropriate matrix. Standard curves were performed in duplicate and included halomon concentrations of 0.01, 0.03, 0.1, 0.3, 1.0, 3.0, and 10 µg/ml.

No decomposition was observed in 1.0- or 7.5-µg/ml solutions of halomon prepared in mouse plasma and stored at 37 °C for 1, 2, 4, or 24 h. Similarly, following storage at 22 °C for up to 72 h, no decomposition was observed in toluene extracts prepared from mouse plasma containing halomon at 0.3, 3, or 10 µg/ml. There was no endogenous material in mouse plasma, mouse tissues, diluent 12, or sesame oil that interfered with the determination of halomon or internal standard (Fig. 2). In plasma the limit of quantitation [23] was 0.01 µg/ml, and the assay was linear between 0.01 and 10 µg/ml. In tissues the limit of quantitation was 0.03 µg/g and the assay was linear to 10 µg/g [23]. Recoveries from spiked samples of plasma ($n = 3$) were 82–87% at low (0.3 µg/ml) and at higher concentrations (10 µg/ml). Recovery of halomon from various tissues was of the same order of magnitude. The coefficient of variability for the analysis in plasma was $\leq 15\%$ with regard to both intraday analysis of any concentration on the standard curve or interday comparison of standard curves.

Pharmacokinetic analysis

Time courses of plasma concentrations of halomon versus time were analyzed by both noncompartmental and compartmental methods. The area under the curve from zero to infinity (AUC) and the terminal half-life ($t_{1/2}$) were estimated by noncompartmental analysis with the LaGrange function [26] as implemented by the LAGRAN computer program [22]. Total body clearance (CL_{tb}) was calculated from the definition:

$$CL_{tb} = \frac{Dose}{AUC},$$

and the steady-state volume of distribution (Vd_{ss}) was calculated from the formula:

$$Vd_{ss} = Cl_{tb}/k_{el}.$$

In addition, individual concentrations of halomon detected in plasma versus time were fit to compartmental models with the program ADAPT II [8] using generalized least-squares estimation. Two- and three-compartment, open linear models were fit to studies in which halomon was delivered i.v. Similar models with first-order absorption processes were employed in studies wherein halomon was delivered i.p., s.c., or by enteral gavage. Model discrimination was based on Akaike's information criteria (AIC) [1], defined as:

$$AIC = 2p + n(lnWSSR),$$

where p represents the number of parameters in the model, n equals the number of observations, and $WSSR$ represents the weighted sum of square residuals.

After it was determined that the two-compartment, open linear model was most suitable, the four i.v. studies that had been modeled individually were also modeled simultaneously, with each being treated as a separate bolus in a multiple-dosing regimen and with each dose being separated by a time sufficient for washout without carryover from the previous dose [10]. This time was set at 3,000 min. Mean values and standard deviations for individual parameters determined by a standard two-stage analysis [13] of the four individually modeled i.v. studies were then compared with the respective mean values and standard deviations produced by the simultaneous modeling.

Results

Plasma pharmacokinetics

Because no information was available with regard to the toxicity of halomon after i.v. administration to mice, preliminary efforts were directed at defining

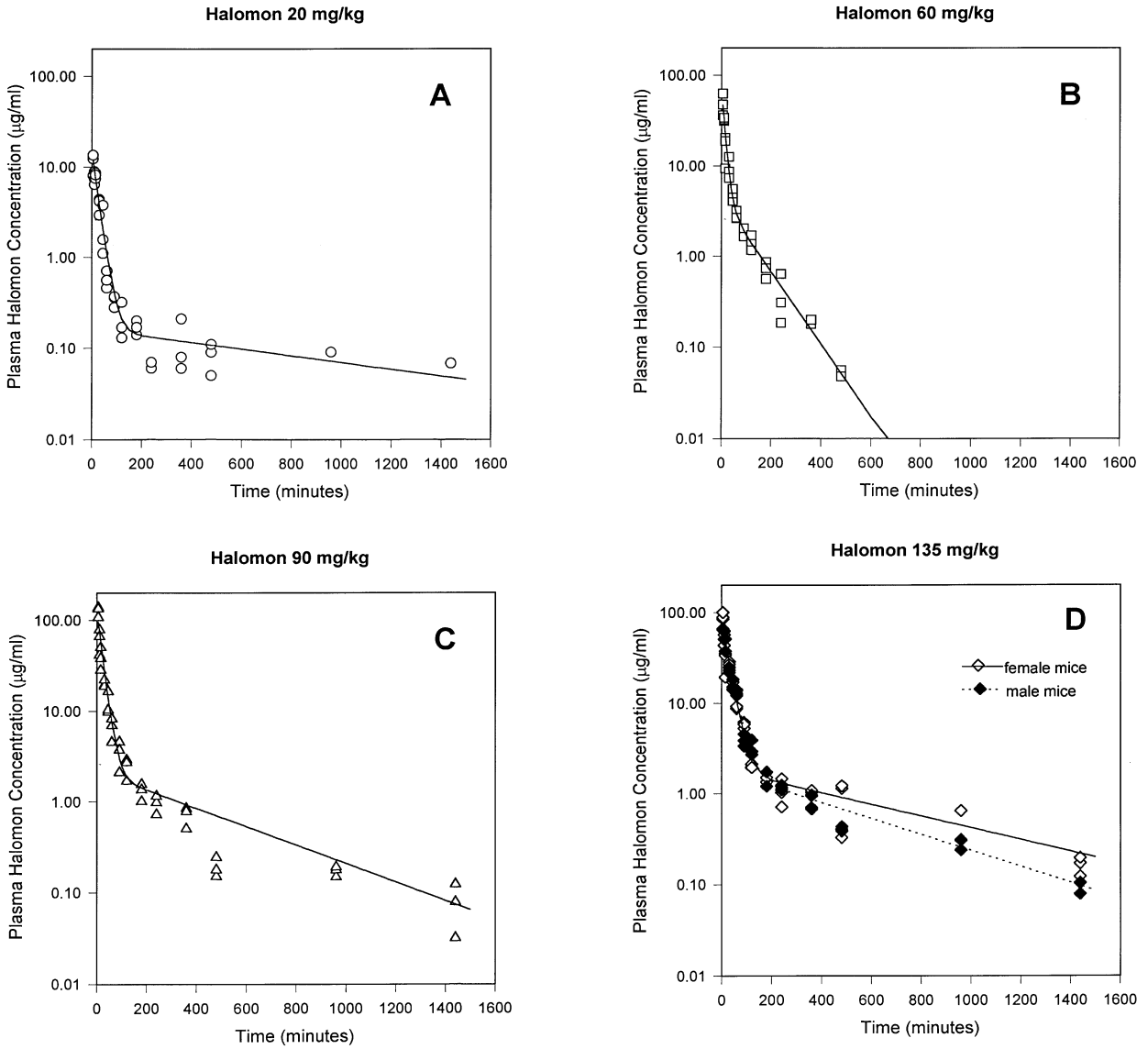

Fig. 3 A–D Concentrations of halomon detected in the plasma of female CD_2F_1 mice given i.v. bolus doses of A 20 (*circles*), B 60 (*squares*), C 90 (*triangles*), or D 135 mg/kg (*white diamonds*) and of D male CD_2F_1 mice injected with an i.v. bolus dose of 135 mg/kg (*black diamonds*). *Symbols* represent halomon concentrations measured in the plasma of individual mice. *Curves* represent fits of the data to a two-compartment, open linear model

a suitably high but nonlethal i.v. dose. Halomon was dissolved in diluent 12 : 0.154 *M* NaCl (1 : 3, v : v). Doses of 200, 135, or 90 mg/kg were delivered in a maximal volume of 10 ml/kg to groups of five female CD_2F_1 mice. All five mice injected with a halomon dose of 200 mg/kg were dead at 28 h after injection, but all of the control mice injected only with vehicle survived with no adverse effect. All mice given 200 mg/kg exhibited hepatic lesions, including moderate centrilobular degeneration and congestion as well as mild periportal cytoplasmic vacuolation and moderate numbers of necrotic hepatocytes. Other organs in these mice appeared normal. All mice injected with a halomon dose of 135 mg/kg survived, as did all five mice injected with a dose of 90 mg/kg.

On the basis of the above-mentioned observations, 135 mg/kg was selected as the highest dose to be used in studies investigating the pharmacokinetics and tissue distribution of halomon after i.v. administration (Fig. 3) as well as the dose to be used in studies on the bioavailability of halomon after i.p., s.c., or enteral delivery (Fig. 4). Subsequent i.v. studies using sequential one-third (90 mg/kg, 60 mg/kg) or two-thirds (20 mg/kg) dose reductions were undertaken to evaluate the linearity of halomon pharmacokinetics over a reasonably broad yet relevant range of doses (Fig. 3).

The i.v. bolus delivery of halomon at a dose of 135 mg/kg produced "peak" plasma halomon concentrations of between 85 and 100 μg/ml in female mice and between 65 and 67 μg/ml in male mice killed at

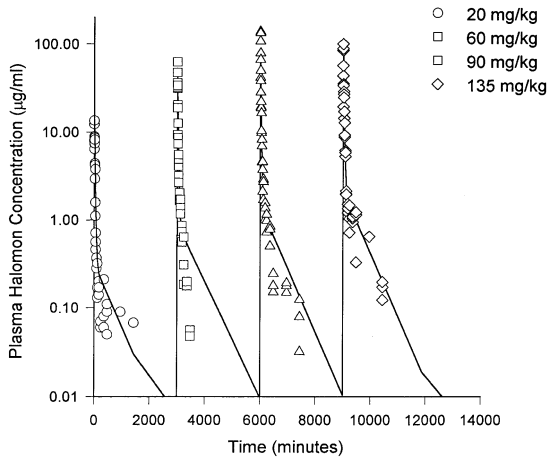

Fig. 4 Simultaneous fitting of a two-compartment, open linear model to concentrations of halomon detected in the plasma of female CD_2F_1 mice given i.v. bolus doses of 20 (*circles*), 60 (*squares*), 90 (*triangles*), or 135 mg/kg (*diamonds*). *Symbols* represent halomon concentrations measured in the plasma of individual mice. *Curves* represent fits of the data to a two-compartment, open linear model

5 min after injection (Fig. 3). In female mice, sequential reduction of the halomon dose to 90, 60, and, finally, 20 mg/kg resulted in "peak" plasma halomon concentrations ranging between 108 and 139, between 33 and 63, and between 8 and 14 μg/ml, respectively (Fig. 3).

Noncompartmental analysis (Table 1) of the curves of plasma halomon concentration versus time (Fig. 3) produced by i.v. administration showed the pharmacokinetics of halomon to be linear over the range of 20–135 mg/kg, as the AUC changed proportionally with the dose (Table 1). As indicated by the proportional relationship between the halomon dose and the AUC, CL_{tb} remained between 36 and 56 ml min^{-1} kg^{-1} and did not vary systematically across the nearly 7-fold range of doses studied (Table 1). The i.v. bolus delivery of a halomon dose of 135 mg/kg to male CD_2F_1 mice produced an AUC of 2,674 μg ml^{-1} min as compared with the AUC of 3,166 μg ml^{-1} min calculated when the same dose was given to female mice. However, the CL_{tb} calculated for male mice treated i.v. with 135 mg/kg was similar to the values calculated for female mice treated i.v. with halomon doses of 20 or 60 mg/kg and was not significantly different from the mean CL_{tb} calculated for the four doses used in i.v. studies in female mice (Table 1).

Compartmental modeling of the curves of plasma halomon concentration versus time (Fig. 3) produced by i.v. bolus delivery of halomon showed the data to be best fit by a two-compartment, open linear model (Fig. 3, Table 2). For every dose the weighted sums of square residuals for two- and three-compartment models were nearly identical. Thus, addition of a third compartment produced no improvement in model fit over that provided by the simpler two-compartment model, and the additional mathematical complexity resulted in a less favorable AIC. Therefore, the two-compartment model was selected as most appropriate for these data. The individual model parameters resulting from fitting of a two-compartment, open linear model to the plasma halomon concentration versus time data from i.v. studies in female mice are displayed in Table 2, as are the values for $t_{1/2\alpha}$, $t_{1/2s}$, CL_{tb}, and Vd_{ss} that were derived from these parameters.

In an attempt to address this issue with a different approach, we employed the much more computationally intensive method of simultaneous modeling to a two-compartment, open linear model the plasma concentration data from individual female mice treated at all four dose levels (Fig. 4). For this compartmental modeling the dosing events of 20, 60, 90, and 135 mg/kg were separated by 3,000 min, a period sufficient for the plasma halomon concentration resulting from the previous dosing event to be negligible. This approach produced mean values for k_{10}, k_{12}, k_{21}, and V that were very similar to those calculated with the standard two-stage approach, although the standard deviation for each parameter was much lower than that produced with the standard two-stage approach (Table 2). The individual model parameters and derived pharmacokinetic parameters resulting from fitting of a two-compartment, open linear model to the plasma halomon concentration versus time data from male mice given an i.v. dose of 135 mg/kg were similar to

Table 1 Noncompartmental pharmacokinetic analyses of halomon plasma concentration versus time curves (*NA Not applicable*)

Dose (mg/kg)	Route	Sex	AUC (μg ml^{-1} min)	F[a] %	k_{el} (min^{-1})	$t_{1/2}$ (min)	Vd_{ss} (ml/kg)	CL_{TB} (ml min^{-1} kg)
20	i.v.	F	411		0.00055	1,252	21,800	48.6
60	i.v.	F	1,074		0.00188	370	9,010	55.9
90	i.v.	F	2,533		0.00187	371	4,500	35.5
135	i.v.	F	3,166		0.00137	507	13,100	42.6
135	i.p.	F	1,427	45	0.00094	739	76,400[b]	NA
135	s.c.	F	1,488	47	0.00144	480	49,100[b]	NA
135	p.o.	F	118	4	0.00256	271	463,000[b]	NA
135	i.v.	M	2,674		0.00148	472	9,710	50.5

[a]The fraction of the dose that is bioavailable
[b]Apparent Vd_{ss}

Table 2 Compartmental pharmacokinetic analyses of halomon plasma concentration versus time curves (*NA* Not applicable)

Dose (mg/kg)	Route	Sex	k_a (min^{-1})	k_{10} (min^{-1})	k_{12} (min^{-1})	k_{21} (min^{-1})	Vc (ml/kg)	$t_{1/2\alpha}$ (min)	$t_{1/2\beta}$ (min)	CL (ml min^{-1} kg^{-1})	Vd_{ss} (ml/kg)
20[a]	i.v.	F	NA	0.0285	0.0161	0.0013	1,382	15.4	817	39.3	17,930
60	i.v.	F	NA	0.0536	0.0212	0.0136	882	8.8	76	47.2	2,262
90	i.v.	F	NA	0.0372	0.0127	0.0032	733	13.7	297	27.2	3,650
135	i.v.	F	NA	0.0242	0.0119	0.0023	1,596	18.8	467	38.6	9,971
			Mean	0.0359	0.0155	0.0051	1,148	14.2	414	38.1	8,453
			SD	0.013	0.0042	0.0057	408	4.2	313	8.2	7,153
20–135	i.v.	F	NA	0.031	0.0132	0.0024	1,059	15.4	421	32.8	6,903
			SD	0.0015	0.001	0.00015	73	3.1	4	1.2	566
135	i.v.	M	NA	0.024	0.008	0.0028	1,812	21.2	343	43.4	7,065
135	i.p.	F	0.04	0.005	0.004	0.0013	13,710	72.2	1,052	68[c]	57,000[d]
135	s.c.	F	0.036	0.0006	0.024	0.0095	15,510	18.3	471	90.9[c]	54,600[d]
135	p.o.	F	0.097	0.017	0.074	0.0087	41,610	30.4	460	705.4[c]	394,200[d]

[a] All parenteral doses were formulated in 1 part diluent 12 and 3 parts 0.154 *M* NaCl, and the enteral dosing solution was formulated in 1 part diluent 12 and 3 parts distilled water
[b] Data from all animals treated i.v. with doses of 20, 60, 90, and 135 mg/kg were modeled simultaneously as described in Materials and methods
[c] Apparent CL
[d] Apparent Vd_{ss}

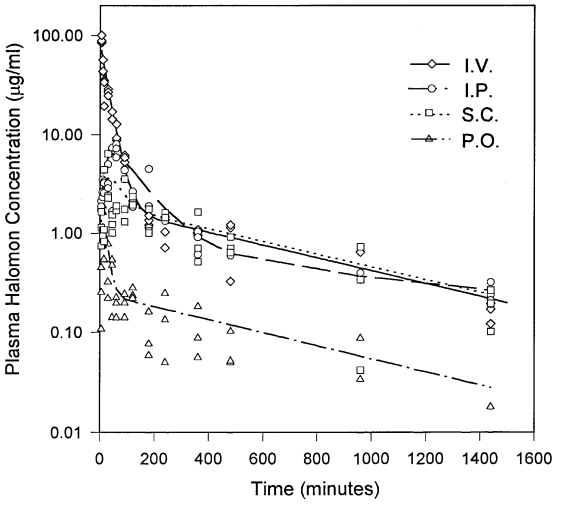

Fig. 5 Concentrations of halomon detected in the plasma of female CD_2F_1 mice given 135-mg/kg bolus doses of halomon by the i.v. (*diamonds*), i.p. (*circles*), s.c. (*squares*), or enteral (*triangles*) route. *Symbols* represent halomon concentrations measured in the plasma of individual mice. *Curves* represent fits of the data to a two-compartment, open linear model with first-order absorption

those produced by fitting of the data from female mice (Table 2).

The i.p. delivery of 135 mg/kg of halomon formulated in diluent 12 and 0.154 *M* NaCl produced detectable plasma halomon concentrations within 5 min, and peak plasma halomon concentrations of 5–8 µg/ml occurred at between 30 and 60 min after injection (Fig. 5). At between 60 and 1,440 min, plasma halomon concentrations declined progressively, but they remained above the lower limit of quantitation even at 1,440 min. When analyzed in a noncompartmental manner, these plasma halomon concentration versus time data produced an AUC of 1,427 µg ml^{-1} min, corresponding to a bioavailability of 45% (Table 1). The time course of plasma halomon concentrations associated with i.p. administration of a 135-mg/kg dose formulated in diluent 12 and 0.154 *M* NaCl was also described by a two-compartment, open linear model with first-order absorption from the peritoneal cavity (Fig. 5, Table 2).

The i.p. delivery of a 135-mg/kg dose of halmon formulated in sesame oil produced a plasma concentration versus time profile that was very different from that observed after i.p. delivery of the same dose of drug formulated in diluent 12 and 0.154 *M* NaCl. In this case, very low plasma concentrations of halomon were detected at 5 min after i.p. administration, and peak plasma halomon concentrations of 0.2–0.6 µg/ml occurred at between 15 and 45 min. Thereafter, plasma halomon concentrations remained almost constant at approximately 0.2 µg/ml for the duration of the study, with no appreciable decline being observed between 60 and 1,440 min. Although these data did not lend themselves to either compartmental or noncompartmental modeling, the maintenance of a relatively constant plasma concentration of halomon implied zero-order absorption of halomon from the peritoneal cavity at a rate that could be calculated by rearranging the relationship:

$$(\textit{Steady-state concentration}) = (\textit{Rate of delivery})/(\textit{Clearance}).$$

Using a mean steady-state halomon concentration calculated to be 0.21 µg/ml, a mean CL_{tb} of 38 ml min^{-1}

Table 3 Concentrations of halomon detected in plasma and tissues of female CD_2F_1 mice injected i.v. with a 135-mg/kg dose of halomon. Data represent mean values ±SD for three mice (*Sk. Musc.* Skeletal muscle, *ND* not detectable)

Time (min)	Plasma (μg/ml)	Brain (μg/g)	Heart (μg/g)	Lungs (μg/g)	Liver (μg/g)	Kidney (μg/g)	Spleen (μg/g)	Sk. Musc. (μg/g)	Fat (μg/g)
5	91.5 ± 8.1	62.7 ± 1.0	187.2 ± 13.7	96.2 ± 2.0	61.0 ± 26.3	64.1 ± 3.0	42.6 ± 7.9	41.0 ± 19.0	27.6 ± 9.6
10	48.2 ± 7.9	64.6 ± 3.8	58.4 ± 33.6	64.4 ± 25.1	34.9 ± 30.0	58.7 ± 10.7	23.7 ± 8.3	30.0 ± 11.1	37.7 ± 9.8
15	29.6 ± 8.8	46.2 ± 5.3	49.8 ± 13.3	39.7 ± 11.6	10.5 ± 6.2	48.5 ± 7.5	12.2 ± 3.7	26.5 ± 12.7	43.9 ± 24.9
30	27.0 ± 2.0	67.3 ± 4.4	36.2 ± 14.9	46.4 ± 11.0	25.2 ± 16.6	38.2 ± 10.2	11.9 ± 1.5	27.9 ± 24.6	74.4 ± 6.6
45	15.4 ± 1.6	38.4 ± 3.9	37.7 ± 35.2	42.1 ± 14.0	9.7 ± 10.5	37.1 ± 12.4	6.0 ± 0.06	35.9 ± 31.5	55.5 ± 12.0
60	10.3 ± 2.2	34.4 ± 6.6	34.0 ± 16.1	22.2 ± 4.4	7.8 ± 9.3	29.5 ± 5.3	5.4 ± 1.6	38.2 ± 31.9	77.8 ± 15.3
90	5.8 ± 0.5	12.7 ± 5.4	11.9 ± 9.2	21.5 ± 1.0	1.6 ± 1.7	25.2 ± 8.4	2.9 ± 1.6	26.7 ± 4.6	70.7 ± 26.7
120	2.0 ± 0.1	4.8 ± 1.0	4.4 ± 1.2	10.8 ± 3.9	0.5 ± 0.1	15.5 ± 8.4	2.4 ± 0.6	22.7 ± 19.4	63.2 ± 13.5
180	1.4 ± 0.2	2.0 ± 0.0	5.6 ± 4.6	11.0 ± 3.6	0.2 ± 0.1	13.7 ± 4.0	2.5 ± 1.0	11.6 ± 8.8	67.7 ± 5.0
240	1.1 ± 0.4	0.8 ± 0.1	2.3 ± 1.7	5.7 ± 3.1	0.3 ± 0.2	17.4 ± 10.6	2.7 ± 1.5	15.8 ± 9.2	65.9 ± 11.7
360	1.0 ± 0.1	0.5 ± 0.2	2.1 ± 2.2	3.5 ± 1.7	0.2 ± 0.3	12.8 ± 8.1	1.0 ± 0.4	5.2 ± 3.2	68.0 ± 7.1
480	0.9 ± 0.5	0.3 ± 0.1	2.0 ± 1.4	2.2 ± 0.3	0.5 ± 0.9	6.9 ± 7.8	0.4 ± 0.1	3.3 ± 1.8	65.1 ± 6.1
960	0.2 ± 0.4	0.3 ± 0.0	1.3 ± 1.4	0.9 ± 0.7	1.2 ± 0.7	4.6 ± 2.0	0.5 ± 0.3	4.2 ± 2.1	59.8 ± 5.1
1,440	0.2 ± 0.0	0.1 ± 0.0	0.5 ± 0.3	0.3 ± 0.0	ND	2.2 ± 0.9	0.4 ± 0.3	1.5 ± 0.9	52.0 ± 6.4

kg^{-1}, and an average mouse weight in these studies of 0.0175 kg, a rate of absorption of 0.14 μg/min was calculated.

The s.c. delivery of a 135-mg/kg dose of halomon formulated in diluent 12 and 0.154 *M* NaCL produced detectable plasma concentrations of halomon within 5 min, and peak plasma halomon concentrations of 2–6 μg/ml occurred at between 15 and 30 min after injection (Fig. 5). Thereafter, plasma halomon concentrations declined progressively, but at 1,440 min they remained above the lower limit of quantitation of the gas-chromatography assay employed. Noncompartmental analysis of these plasma halomon concentration versus time data produced an AUC of 1,488 μg ml^{-1} min, corresponding to a bioavailability of 47% (Table 1). The time course of plasma halomon concentrations produced by s.c. delivery of 135 mg/kg could also be fit to a two-compartment, open linear model with first-order absorption (Fig. 5, Table 2).

Enteral administration by gavage of a 135-mg/kg dose of halomon formulated in diluent 12 and distilled water produced low but detectable concentrations of halomon in plasma by 5 min after drug delivery. Peak plasma halomon concentrations of 1–2 μg/ml occurred at 10 min after drug delivery and declined thereafter such that in some mice studied at 960 and 1,440 min, plasma halomon concentrations were below the lower limit of quantitation (Fig. 5). Noncompartmental analysis of these plasma halomon concentration versus time data produced an AUC of 118 μg ml^{-1} min, corresponding to a bioavailability of 4% (Table 1). As found in the i.p. and s.c. studies, the time course of plasma halomon concentrations produced by enteral delivery of a 135-mg/kg dose could be fit to a two-compartment, open linear model with first-order absorption from the gastrointestinal tract (Fig. 5, Table 2)

Urinary excretion of halomon

Minimal amounts of halomon were detected in the urine of mice. In groups of mice injected i.v. with 135 mg/kg, between 0.0034% and 0.0046% of the delivered dose was accounted for by urinary excretion of the parent compound in the first 24 h after injection. In mice injected i.v. with 90 mg/kg, urinary excretion of the parent compound accounted for 0.0058% of the delivered dose.

Tissue halomon concentrations following i.v administration

After its i.v. bolus delivery at a dose of 135 mg/kg to female or male mice, halomon was distributed to all tissues (Tables 3, 4). Noteworthy were the observations that brain concentrations of halomon were comparable with concomitant concentrations detected in plasma and most other tissues and that halomon had relatively limited access to the testes. Also, whereas the halomon concentrations detected in most tissues declined in parallel with those measured in plasma, the concentrations of halomon found in fat exceeded those observed in all other tissues by 30 min after injection and remained essentially constant for the duration of the study (Tables 3, 4). Finally, there were relatively low concentrations of halomon in the livers of both female and male mice (Tables 3, 4).

Discussion

Halomon, a natural product isolated from red algae [12], possesses a number of characteristics that make it an interesting candidate for development as an

Table 4 Concentrations of halomon detected in plasma and tissues of male CD_2F_1 mice injected i.v. with a 135-mg/kg dose of halomon. Data represent mean values ± SD for three mice (*Sk. Musc.* Skeletal muscle)

Time (min)	Plasma (μg/ml)	Brain (μg/g)	Heart (μg/g)	Lungs (μg/g)	Liver (μg/g)	Kidney (μg/g)	Spleen (μg/g)	Sk. Musc. (μg/g)	Fat (μg/g)	Testes (μg/g)
5	65.9 ± 0.8	66.2 ± 17.0	206.0 ± 6.6	96.8 ± 1.8	92.8 ± 23.8	66.5 ± 1.8	80.1 ± 2.8	31.0 ± 12.5	55.1 ± 30.6	5.3 ± 0.6
10	58.9 ± 6.8	78.8 ± 6.6	127.0 ± 37.3	85.6 ± 15.7	179.5 ± 41.2	50.7 ± 2.2	32.2 ± 10.4	26.3 ± 5.3	75.3 ± 9.0	7.6 ± 3.5
15	35.0 ± 18.0	54.1 ± 18.9	86.6 ± 51.8	48.1 ± 21.4	72.1 ± 90.1	26.2 ± 7.8	14.9 ± 6.1	13.0 ± 3.5	71.5 ± 52.9	5.0 ± 3.4
30	23.5 ± 1.6	40.6 ± 14.0	36.8 ± 16.4	43.5 ± 4.0	46.2 ± 22.1	25.7 ± 9.4	9.1 ± 2.5	23.4 ± 12.9	100.1 ± 7.3	8.3 ± 3.0
45	16.0 ± 2.3	26.4 ± 6.3	21.3 ± 7.5	33.6 ± 12.6	87.1 ± 25.2	31.8 ± 9.5	9.3 ± 2.0	19.4 ± 7.8	91.3 ± 9.5	6.9 ± 1.3
60	13.4 ± 1.0	24.5 ± 3.5	11.7 ± 3.0	29.6 ± 1.5	26.9 ± 17.9	25.9 ± 13.4	6.0 ± 0.3	10.7 ± 7.0	105.3 ± 7.5	10.1 ± 6.8
90	4.0 ± 3.22	10.4 ± 5.5	4.8 ± 2.0	20.0 ± 8.5	2.0 ± 0.5	31.6 ± 25.0	4.6 ± 0.4	9.6 ± 5.5	95.5 ± 5.7	9.6 ± 4.7
120	3.22 ± 0.6	4.9 ± 2.4	4.6 ± 0.8	11.7 ± 0.8	1.7 ± 1.5	16.4 ± 7.0	3.5 ± 0.8	8.5 ± 4.2	86.0 ± 30.6	8.3 ± 6.4
180	1.6 ± 0.3	1.2 ± 0.8	3.7 ± 3.0	12.4 ± 1.1	2.8 ± 2.8	10.0 ± 4.7	3.8 ± 2.1	20.0 ± 23.8	104.4 ± 3.2	5.4 ± 2.7
240	1.2 ± 0.1	1.0 ± 0.5	2.6 ± 2.7	6.2 ± 2.3	0.8 ± 0.2	16.6 ± 13.1	2.1 ± 0.4	4.8 ± 2.5	96.0 ± 1.9	4.2 ± 1.3
360	0.8 ± 0.2	0.5 ± 0.0	2.4 ± 1.6	3.9 ± 1.2	0.5 ± 0.1	14.7 ± 3.4	1.5 ± 0.3	14.8 ± 10.6	96.0 ± 1.5	7.1 ± 3.7
480	0.4 ± 0.0	0.2 ± 0.1	1.6 ± 1.9	2.9 ± 0.6	0.5 ± 0.2	11.7 ± 8.7	1.8 ± 0.8	6.2 ± 2.2	76.2 ± 15.6	7.1 ± 4.5
960	0.3 ± 0.0	0.3 ± 0.2	0.7 ± 0.4	1.7 ± 0.7	0.3 ± 0.0	5.3 ± 3.9	1.1 ± 0.8	17.3 ± 2.9	84.8 ± 1.7	8.3 ± 5.1
1,440	0.1 ± 0.0	0.2 ± 0.0	0.1 ± 0.1	1.2 ± 0.3	0.1 ± 0.2	0.8 ± 0.4	0.3 ± 0.2	2.2 ± 1.2	57.4 ± 21.2	3.2 ± 2.2

antineoplastic chemotherapeutic agent [4, 11, 21]. The studies described in the current paper are the result of a desire to incorporate more fully the pharmacology of halomon into its in vivo activity and toxicity testing and to develop data that might be useful, should the compound progress to clinical testing. A number of the results described should prove useful in the achievement of these goals.

Demonstration that halomon, which is not very soluble in aqueous solvents, can be formulated in a mixture of diluent 12 and 0.154 *M* NaCl means that in vivo studies of halomon can employ a vehicle used in the formulation of clinically available drugs such as paclitaxel.

The gas-chromatography method developed to quantify halomon in the plasma and tissues of mice has a number of desirable characteristics that should allow its broader application as the development of halomon progresses. The method, which uses electron-capture detection, is sensitive and selective, involves simple sample preparation without costly reagents, uses standard instrumentation that is available in most analytical chemical facilities, and lends itself to automated sample injection and data handling. Each of these properties should facilitate the implementation of the method in other laboratories and allow its application to large numbers and a wide variety of samples.

A number of aspects of the pharmacokinetics studies performed should prove useful in the development of halomon as an antitumor agent. Specifically, the results of these studies will be helpful in interpretation of the results of in vivo toxicity and activity testing of halomon and could be important in the planning of clinical protocols involving the compound. The plasma pharmacokinetics studies of halomon provide reasonable confidence in the linearity of the plasma pharmacokinetics of the drug after i.v. delivery and provide quantitative data with regard to the peak plasma halomon concentrations and durations spent above various plasma thresholds that are produced by several doses of halomon. These data could prove useful in the planning of initial doses and dose-escalation schemes, should halomon be introduced into phase I clinical trials.

Although a complete acute-toxicity study was not performed to define accurately the dose of halomon lethal to 10% of mice (LD_{10}), our preliminary toxicity observations argue against a validated LD_{10} that would be substantially higher than the 135-mg/kg dose used as our high i.v. dose. Therefore, the pharmacokinetic data presented could be extrapolated if pharmacokinetically guided dose escalation [6, 7] were desired. The demonstration of 45–50% bioavailability for the drug delivered i.p. or s.c. implies that these routes could be applicable in in vivo testing. These options, which are much less time-consuming than i.v. drug delivery, could greatly facilitate or simplify the evaluation of halomon. The demonstration of the very low bioavailability of halomon after enteral administration should preclude that as a practical route for preclinical testing and argues against consideration of the development of an oral formulation for clinical evaluation. Although sesame oil has been proposed as a possible vehicle for use in studies of i.p.-delivered halomon, the data from the current studies show the plasma concentrations achieved with this vehicle and route to be extremely low, albeit sustained.

The impetus for undertaking compartmental modeling of halomon plasma concentration versus time data was to develop a model that would be useful in the simulation and prediction of concentration versus time profiles produced by a variety of routes, schedules, and doses employed in in vivo activity and toxicity testing. To do so would require not only an appropriate structural model but also reliable estimates of mean values and standard deviations for the pharmacokinetic

parameters in such a model. As a first step in producing those values, a standard two-stage approach [13] was applied, wherein the mean values and standard deviations were calculated for k_{10}, k_{12}, k_{21}, and V using the values resulting from individually modeled studies of 20-, 60-, 90-, and 135-mg/kg doses (Table 2). The computationally intensive, simultaneous modeling of plasma halomon concentrations in the female mice treated in the four studies in which halomon doses of 135, 90, 60, and 20 mg/kg were given by i.v. injection represents an interesting and relatively novel approach to the analysis of such data [10].

That similar mean values were produced for each pharmacokinetic parameter by the standard two-stage and simultaneous modeling approaches to data analysis increases confidence in those parameter values. The simultaneous modeling procedure minimizes interstudy variability, and the smaller standard deviations produced by this approach likely reflect the minimal intersubject variability expected in a genetically homogeneous population. The larger standard deviations produced by the standard two-stage approach not only incorporate the underlying intersubject variability but also reflect interstudy and experimental variability. Parameter estimates produced by both approaches may be useful. The mean values and standard deviations produced by the simultaneous modeling approach may be most appropriate for use in producing data simulations and predictions for halomon delivered by specified dose and administration schedules to CD_2F_1 mice. The mean values and standard deviations produced by the standard two-stage approach, which reflect additional experimental variability, may be more appropriate for use in comparative studies with other strains of mice or other species.

The tissue-distribution data presented have several implications for the evaluation of in vivo testing of halomon. The wide and rapid tissue distribution of the drug implies good access to implanted or de novo tumors. The tissue concentrations achieved after i.v. bolus delivery of 135 mg/kg (Tables 3, 4) can be considered in light of in vitro cytotoxicity testing by the NCI of halomon against NCI-H460 and U-251 cell lines. In these in vitro studies, 6-h periods of exposure to halomon followed by a 1-week growth period were equipotent to 12-, 24-, 48-, or 144-h exposure periods, and halomon concentrations producing 50% inhibition of cell growth or 50% cell kill ranged from 3 to 6 μg/ml for U-251 cells and from 5 to 18 μg/ml for H460 cells. The ability of halomon to achieve substantial concentrations in the brain raises the potential applicability of halomon in the treatment of CNS malignancies. The remarkable persistence of halomon in fat might be expected due to the lipophilic nature of the drug and the multiple halogens incorporated into its structure. Other compounds that share these structural features, such as anesthetics [16], pesticides [15], and antitumor agents [25], are known to be concentrated and persist in fat.

Whereas the plasma pharmacokinetic data presented have allowed the development of a population pharmacokinetic model for the simulation of plasma halomon concentrations expected after i.v. delivery, the availability of concomitant concentrations of halomon in plasma and multiple tissues at multiple times has allowed the development of a physiologic flow model [2, 3, 5] of the compound [9]. Such a model will allow the simulation of tissue concentrations associated with various doses and schedules of halomon administration and should also be applicable for species scale-up in simulatons of the pharmacokinetics of the compound in other, larger species such as humans [18–20].

Several other aspects of the data presented warrant discussion. The observations that urinary excretion of halomon was negligible and that hepatic concentrations of the compound decreased rapidly and were relatively low as compared with those measured in other tissues and plasma argue for either biliary excretion or, more likely, hepatic metabolism as the major route of halomon elimination. The importance of hepatic cytochrome P450 2E1 in the metabolism of halogenated compounds is well recognized [14, 17]. We are actively evaluating whether this specific P450 or any other is involved in halomon metabolism. The potential implications of such metabolism in the mechanisms of action and toxicity of halomon remain to be defined. Whether murine metabolism of halomon is an adequate model for human metabolism of the compound also remains to be defined.

Other unanswered questions and caveats associated with the current studies include those as to whether the 20% increase in clearance of the compound noted in the one study performed in male mice is reproducible and how different the pharmacokinetics of halomon might be in other strains of mice or in mice bearing tumors. These issues, although obviously relevant to a complete appreciation of the pharmacology of halomon, have been deferred for practical and logistic reasons until more data on the in vivo activity and toxicities of halomon have been defined.

Acknowledgements We appreciate the encouragement of Dr. Kimberly Duncan and her confidence in our ability to carry out this work. We also gratefully acknowledge the assistance of Dr. Sung Kim in developing the gas-chromatography assay used in this work, the excellent technical assistance of Eleanor G. Zuhowski in some animal studies, and the excellent secretarial assistance of Helen Spiker in the preparation of this manuscript.

References

1. Akaike H (1979) A Bayesian extension of the minimal AIC procedures of autoregressive model fitting. Biometrika 66:237
2. Bischoff KB (1967) Applications of a mathematical model for drug distribution in mammals. In: Hershey D (ed) Chemical engineering in medicine and biology. Plenum, New York, p 417
3. Bischoff KB, Brown RG (1966) Drug distribution in mammals. Chem Eng Prog Symp Ser 62:32

4. Boyd MR, Paull KD, Rubinstein LR (1992) Data display and analysis strategies for the NCI disease-oriented in vitro antitumor drug screen. In: Valeriote FA, Corbett T, Baker L (eds) Cytotoxic anticancer drugs: models and concepts for drug discovery and development. Kluwer, Amsterdam, p 11
5. Chen H-SG, Gross JF (1979) physiologically based Pharmacokinetic models for anticancer drugs. Cancer Chemother Pharmacol 2:85
6. Collins JM, Zaharko DS, Dedrick RL, Chabner BA (1986) Potential roles for preclinical pharmacology in phase I trials. Cancer Treat Rep 70:73
7. Collins JM, Grieshaber CK, Chabner BA (1990) Pharmacologically guided phase I clinical trials based upon preclinical drug development. J Natl Cancer Inst 82:1321
8. D'Argenio DZ, Schumitzky A (1979) A program package for simulation and parameter estimation in pharmacokinetic systems. Comput Methods Prog Biomed 9:115
9. Eiseman JL, Eddington ND, Sentz DL, Rosen DM, Ballesteros MF, Egorin MJ (1996) Tissue distribution and physiological model of halomon in male and female CD2F1 mice. Proc Am Assoc Cancer Res 37 (in press)
10. Eiseman JL, Yuan Z-M, Eddington ND, Senz DL, Callery PS, Egorin MJ (1996) Plasma pharmacokinetics and urinary excretion of the polyamine analogue 1, 19-bis(ethylamino)-5, 10, 15-triazanonadecane in CD_2F_1 mice. Cancer Chemother Pharmacol (in press)
11. Fuller RW, Cardellina JH II, Kato Y, Brinen LS, Clardy J, Snader KM, Boyd MR (1992) A pentahalogenated monoterpene from the red alga *Portieria halomonii* produces a novel cytotoxicity profile against a diverse panel of human tumor cell lines. J Med Chem 35:3007
12. Fuller RW, Cardellina JH II, Jurek J, Scheuer PJ, Alvarado-Lindner B, McGuire M, Gray GN, Steiner JR, Clardy J, Menez E, Shoemaker RH, Newman DJ, Snader KM, Boyd MR (1994) Isolation and structure/activity features of halomon-related antitumor monoterpenes from the red alge *Portieria hornemanii*. J Med Chem 37:4407
13. Grasela TH Jr, Antal EJ, Townsend RJ, Smith RB (1986) An evaluation of population pharmacokinetics in therapeutic trials. I. Comparison of methodologies. Clin Pharmacol Ther 39:605
14. Guengerich FP, Kim D-H, Iwasaki M (1991) Role of human cytochrome P-450 IIE1 in the oxidation of many low molecular weight cancer suspects. Chem Res Toxicol 4:168
15. Hayes WJ Jr (1966) Monitoring food and people for pesticide content. In: Scientific aspects of pest control. Publication 1402, National Academy of Sciences. National Research Council, Washington, D.C., p314
16. Kennedy SK, Longnecker DE (1990) History and principles of anesthesiology. In: Gilman AG, Rall TW, Nies AS, Taylor P (eds) Goodman and Gilman's pharmacologic basis of therapeutics, 8th edn. Pergamon, New York, p 269
17. Koop DR (1992) Oxidative and reductive metabolism by cytochrome P450 2E1. FASEB J 6:724
18. Mordenti J (1985) Pharmacokinetic scale-up: accurate prediction of human pharmacokinetic profiles from animal data. J Pharm Sci 74:1097
19. Mordenti J (1985) Dosage regimen design for pharmaceutical studies conducted in animals. J Pharm Sci 79:852
20. Mordenti J (1986) Man versus beast: pharmacokinetic scaling in mammals. J Pharm Sci 75:1028
21. Paull KD, Shoemaker RH, Hodes L, Monks A, Scudiero DA, Rubinstein L, Plowman J, Boyd MR (1989) Display and analysis of patterns of differential activity of drugs against human tumor cell lines: development of the mean graph and COMPARE algorithm. J Natl Cancer Inst 81:1088
22. Rocci ML, Jusko WJ (1983) LAGRAN program for area and moments in pharmacokinetic analysis. Comput Prog Biomed 16:203
23. Shah VP, Midha KK, Dighe S, McGilvery IJ, Skelly JP, Yacobi A, Layloff T, Viswanathan CE, Cook CE, McDowall RD, Pittman KA, Spector S (1991) Analytical methods validation: bioavailability, bioequivalence and pharmacokinetic studies. Eur J Drug Metab Pharmacokinet 16:249
24. Stallard MO, Faulkner DJ (1974) Chemical constituents of the digestive gland of the sea hare *Aplysia californica*. I. Importance of diet. Comp Biochem Physiol [B] 49:25
25. Van Slooten H, Seters AP van, Smeenk D, Moolenar AJ (1982) O,p'-DDD (mitotane) levels in plasma and tissues during chemotherapy and at autopsy. Cancer Chemother Pharmacol 9:85
26. Yeh KC, Kwan KC (1978) A comparison of numerical integrating algorithms by trapezoidal, LaGrange and Spline approximation. J Pharmacokinet Biopharm 6:79